Generalized direct strength design approach: steel cold-formed columns under buckling mode interaction

Gustavo Yoshio Matsubara[1], Eduardo de Miranda Batista[2]

[1]*COPPE, Civil Engineering Program, Federal University of Rio de Janeiro*
Centro de Tecnologia, Bloco I, sala B101, Ilha do Fundão, CEP 21945-909, Rio de Janeiro/RJ, Brazil.
gustavoyoshio@coc.ufrj.br
[2] *COPPE, Civil Engineering Program, Federal University of Rio de Janeiro*
Centro de Tecnologia, Bloco I, sala B101, Ilha do Fundão, CEP 21945-909, Rio de Janeiro/RJ, Brazil.
batista@coc.ufrj.br

Abstract. Thin-walled steel cold-formed members exhibit local (L), distortional (D), and global (G) buckling modes. These modes can interact in various ways, depending on the relationship between the corresponding buckling loads (P_{crL}, Pc_{rD}, and P_{crG}). The direct strength method (DSM) provides equations for designing columns experiencing global, local, distortional, and local-global buckling interaction (LG). This study focuses on the most general buckling mode interaction (LDG), building upon a recent approach by the authors that covers local-distortional buckling (LD). To develop the design equations, extensive numerical (FEM) and experimental databases were utilized, covering the relevant ranges of slenderness factors (λ_L, λ_D, and λ_G) associated with L, D, and G buckling modes, respectively. The proposed approach combines the existing DSM equations from the Brazilian code NBR 14762:2010 and the design equations for LD buckling interaction, recently proposed by the authors. After identifying the main variables and calibrating the design equations using FEM and literature-based experimental results, the contribution of the global mode is incorporated. The resulting set of design equations takes into account all the possible buckling modes, L, D and G, and the buckling interactions (LG, LD, and LDG) for axial compression of steel cold-formed members.

Keywords: Cold-formed steel member, Local-Distortional buckling interaction, Local-Distortional-Global buckling interaction, Direct Strength Method, Finite Element Method.

1 Introduction

Cold-formed steel (CFS) structural members have gained prominence in metal constructions due to their favorable strength-to-weight ratio. These profiles are manufactured from cold-rolled steel sheets through cold bending, which enhances their strength for structural applications. These bends result in stiffer cross-sectional shapes, with the lipped channel being one of the most common, as depicted in Figure 1. This section-type type allows for the combination of various values for flange width (b_f), web width (b_w), stiffener width (b_s), and thickness (t).

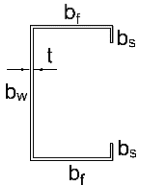

Figure 1 – Cold-formed steel (CFS) lipped channel section.

Depending on the combinations of the cross-section dimensions b_f, b_w, b_s and t, different buckling modes can occur when subjected to axial compression (columns) or bending (beams). Buckling modes can develop as local (L), distortional (D), global (G), or through interaction buckling modes of local-distortional (LD), local-global (LG), distortional-global (DG) and local-distortional-global (LDG) interactions. Some examples of mentioned buckling modes are shown in Figure 2, based on the finite strip method computations with the software FStr [1].

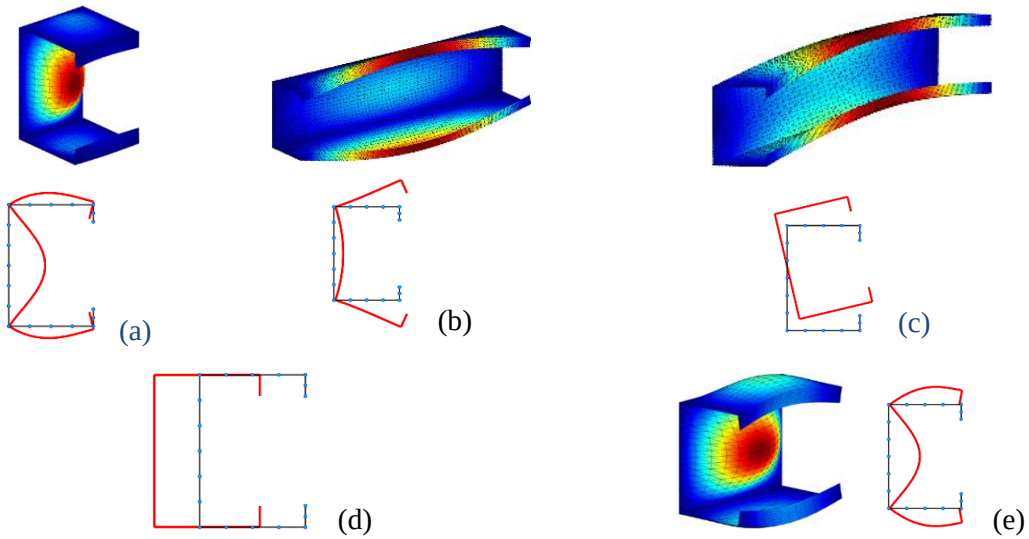

Figure 2 – Steel cold-formed lipped channel column buckling modes, according to FStr software [1]: (a) Local, (b) Distorcional, (c) Global flexural-torsional, (d) Global flexural, (e) Local-Distortional buckling interaction.

The Direct Strength Method (DSM) was proposed by Schafer and Peköz [2], based on earlier studies by Hancock et al. [3], and has been incorporated into the American [4], Australian-New Zealand [5] and Brazilian [6] standards. The DSM provides estimates of the strength of cold formed steel members under axial compression when subjected to global mode (G) - Equation (1), local mode (L) - Equation (2.a), distortional mode (D) - Equation (2.b), and local-global interaction (LG) - Equation (3). The application of this method can be performed with the help of the finite strip (FSM) or the GBT (Generalized beam theory) methods to obtain the critical loads and the associated buckling modes. The elastic buckling analysis can be performed with free access specialized software, such as FStr [1], CUFSM [7] (FSM-based) or GBTUL [8] (GBT-based solution).

Equation (1) related to the global mode column strength, P_{nG}, addresses both minor-axis flexural mode (F_m) and flexural-torsional (FT) mode. This strength Equation is based on the SSRC (Structural Stability Research Council) column curve [4–6,9], using the concept of global slenderness λ_G for design. The column squash load is $P_y = f_y A_g$, where f_y is the steel yield stress and A_g represents the cross-sectional area, and P_G is the critical global buckling load (Fm or FT buckling mode).

$$\chi_n = \begin{cases} \left(0.658^{\lambda_G{}^2}\right) & \lambda_G \leq 1.50 \\ \left(\frac{0.877}{\lambda_G{}^2}\right) & \lambda_G > 1.50 \end{cases} \quad \text{with } \lambda_G = \sqrt{\frac{P_y}{P_G}}, \tag{1.a}$$

$$P_{nG} = \chi_n P_y \tag{1.b}$$

The DSM Equations (2.a) and (2.b) are Winter-type curves, respectively related to the local and distortional buckling column strength, P_{nL}, and P_{nD}. As usual, these strength formulations are dependent on the local and distortional slenderness factor, respectively λ_L and λ_D. The critical load for local and distortional buckling are represented by P_L and P_D, which can be easily accessed by the FStr computational program.

$$P_{nL} = \begin{cases} P_y & \lambda_L \leq 0.776 \\ \left(1 - \frac{0.15}{\lambda_L{}^{0.8}}\right)\frac{P_y}{\lambda_L{}^{0.8}} & \lambda_L > 0.776 \end{cases} \quad \text{with } \lambda_L = \sqrt{\frac{P_y}{P_L}} \tag{2.a}$$

$$P_{nD} = \begin{cases} P_y & \lambda_D \leq 0.561 \\ \left(1 - \frac{0.25}{\lambda_D{}^{1.2}}\right)\frac{P_y}{\lambda_D{}^{1.2}} & \lambda_D > 0.561 \end{cases} \quad \text{with } \lambda_D = \sqrt{\frac{P_y}{P_D}} \tag{2.b}$$

Subsequently, the Direct Strength Method (DSM) incorporated a solution for the local-global interaction (LG), as presented in Equation (3). It is worth noting that this solution indirectly encompasses the pure local mode and pure global mode presented by Equations 2.a and 1, respectively. The ultimate strength P_n using the DSM [5,6,10] is obtained by $P_n = \min\{P_{nLG}; P_{nD}\}$.

$$P_{nLG} = \begin{cases} P_{nG} & \lambda_{LG} \leq 0.776 \\ \left(1 - \frac{0.15}{\lambda_{LG}^{0.8}}\right)\frac{P_{nG}}{\lambda_{LG}^{0.8}} & \lambda_{LG} > 0.776 \end{cases} \qquad \text{with} \qquad \lambda_{LG} = \sqrt{\frac{P_{nG}}{P_L}} \tag{3}$$

2 Finite Element Model for parametric analysis

The parametric analysis was performed with a finite element method (FEM) numerical model, with the commercial software ANSYS [11], incorporating the following considerations:
(i) Quadrilateral SHELL181 elements with 6 degrees of freedom per node and mesh dimensions of 5mm;
(ii) 25mm thick steel plates were attached at the both ends, similar with the experimental tests found in the literature. The degrees of freedom of the plates were all restrained, except for axial displacement, which was allowed for compression application;
(iii) Axial load was applied at the centroid of each end section;
(iv) Plasticity model was bilinear isotropic, von Mises yielding criterion, including hardening effect, according with ANSYS [11] procedures. A tangent modulus of 1450 MPa (0.7% of the Young's modulus E = 210 GPa) was adopted to avoid numerical problems;
(v) The nonlinear analysis was performed using the arc-length method available in the ANSYS v16.0 [11]. This method is suitable to handle with problems that may have one or more points of instability;
(vi) The initial imperfection amplitude adopted was equivalent to 10% of thickness, following the same methodology as proposed by several authors in the literature [12-15]. For columns with significant influence of global mode, a pure global mode with an amplitude equal to L/1000 was implemented, where L represents the length of the column;
(vii) Residual stresses present negligible impact in the ultimate strength and were disregarded as demonstrated in studies by Narayanan and Mahendran [16] and Ellobody and Young [17];
(viii) The rounded corners were also disregarded, as they have little influence on little impact in the ultimate strength [18-19].
The FEM was calibrated with experimental results and allowed testing CFS lipped channel, hat, zed and rack columns displaying LD buckling interaction. Experimental and FEM data were applied to develop the LD buckling interaction solution for the column strength [18], as presented in the next section.

3 Winter-type surface for LD interaction

Based on the parametric numerical study described in section 2 and by Matsubara *et al*. [18], it was proposed the Winter-type curve for CFS lipped channel columns presented in Equation 4. The parameters $\lambda_{maxLD} = \max\{\lambda_L; \lambda_D\}$ and $R_{\lambda DL} = \lambda_D / \lambda_L$ are the main variables to assess the LD buckling interaction.

$$P_{nLD} = \begin{cases} P_y = A_g f_y & \text{for} \quad \lambda_{maxLD} \leq \sqrt[B]{0.5 + \sqrt{0.25 - A}} \\ \left(1 - \frac{A}{\lambda_{maxLD}^{B}}\right)\frac{P_y}{\lambda_{maxLD}^{B}} & \text{for} \quad \lambda_{maxLD} > \sqrt[B]{0.5 + \sqrt{0.25 - A}} \end{cases} \tag{4.a}$$

$$A = \begin{cases} 0.15 & R_{\lambda DL} < 0.80 \\ 0.40\, R_{\lambda DL} - 0.17 & 0.80 \leq R_{\lambda DL} \leq 1.05 \\ 0.25 & R_{\lambda DL} > 1.05 \end{cases} \tag{4.b}$$

$$B = \begin{cases} 0.80 & R_{\lambda DL} < 0.45 \\ -2.26 R_{\lambda DL}^{\,2} + 4.06 R_{\lambda DL} - 0.57 & 0.45 \leq R_{\lambda DL} \leq 1.05 \\ 1.20 & R_{\lambda DL} > 1.05 \end{cases} \tag{4.c}$$

The proposed Equation 4 is related to the strength surface solution shown in Figure 3. It can be noticed that for values of $R_{\lambda DL} \leq 0.45$ and $R_{\lambda DL} \geq 1.05$, the LD interaction is irrelevant and the design procedure converges to the equations related to L and D buckling strength presented in Equations 2.a and 2.b, respectively.
The P_{nLD} validation is summarized in Table 1. The results of the reliability analysis based on the Load and Resistance Factor Design (LRFD) are in good agreement with the safety criteria of both AISI [4] and NBR 14762:2010 [6], respectively $\phi = 0.85$ and $\gamma=1.2$.

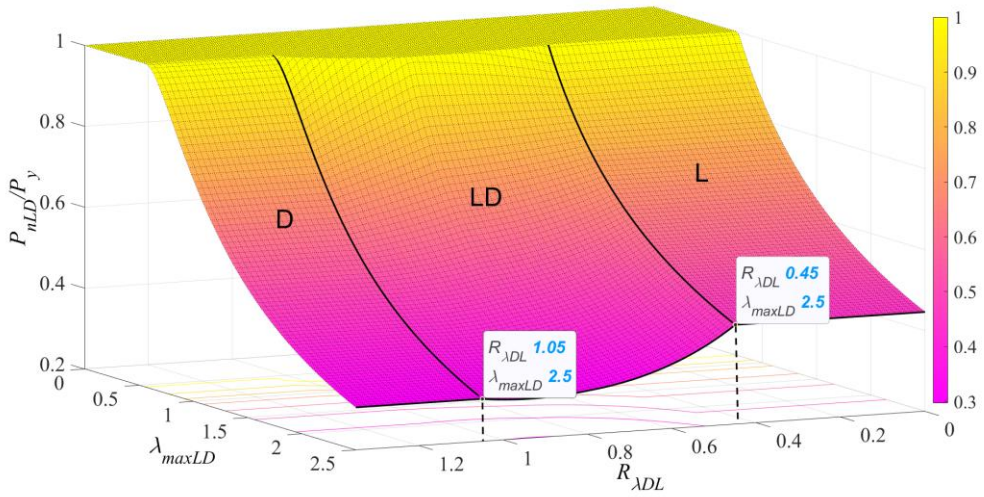

Figure 3: Proposed strength surface for CFS columns developing LD buckling modes interaction.

Table 1. LRFD reliability results of the proposed procedure for CFS columns developing LD buckling interaction, Equation 4. Based on FEM [18,20-23, 32] and experimental [24-31] results.

Section Type		$P_{u,FEM}/P_{nLD}$	P_{EXP}/P_{nLD}	Section Type		$P_{u,FEM}/P_{nLD}$
Lipped Channel	Mean	1.01	0.97	Hat	Mean	1.07
	St. Dev.	0.08	0.08		St. Dev.	0.06
	Coef.Var.	0.08	0.09		Coef.Var.	0,06
	Max	1.26	1.16		Max	1.23
	Min	0.77	0.85		Min	0.87
	Number	611	42		Number	551
	ϕ (γ)	0.90 (1.11)	0.86 (1.16)		ϕ (γ)	0.97 (1.03)
SectionType		$P_{u,FEM}/P_{nLD}$		SectionType		$P_{u,FEM}/P_{nLD}$
Zed	Mean	1.07		Rack	Mean	1.05
	St. Dev.	0.07			St. Dev.	0.10
	Coef.Var.	0.06			Coef.Var.	0.09
	Max	1.27			Max	1.37
	Min	0.85			Min	0.83
	Number	569			Number	595
	ϕ (γ)	0.97 (1.03)			ϕ (γ)	0.93 (1.08)

4 Local-distortional-global buckling modes interaction, LDG

The research on buckling interaction concerning local, distortional and global modes, LDG, has been focused on lipped channel columns [33, 34]. The present study conducted to a new proposition, Equation 5, which gives the column strength P_{nLDG}, incorporating the consideration of the global mode participation through the parameter χ_m, calibrated with FEM results and following the same methodology described in section 2. The column global buckling strength parameter χ_n presented in Equation 1 is considered in Equation 5, and the LDG slenderness

factor is computed as follows, $\lambda_{LDG} = \lambda_{maxLD}\sqrt{\chi_m}$.

$$P_{nLDG} = \begin{cases} P_{nG} = \chi_n P_y & for \quad \lambda_{LDG} \leq \lambda_{limitLDG} \\ \left(1 - \frac{A}{\lambda_{LDG}{}^B}\right)\frac{\chi_m P_y}{\lambda_{LDG}{}^B} & for \quad \lambda_{LDG} > \lambda_{limitLDG} \end{cases} \tag{5.a}$$

$$\lambda_{limitLDG} = \sqrt[B]{0.5\mu + \sqrt{0.25\mu^2 - A\mu}} \quad \text{for } \mu = \frac{\chi_m}{\chi_n} \tag{5.b}$$

$$\chi_m = \begin{cases} \left(C^{\lambda_G{}^D}\right) & \lambda_G \leq 1.50 \\ \left(\frac{E}{\lambda_G{}^F}\right) & \lambda_G > 1.50 \end{cases} \tag{5.c}$$

$$C = \begin{cases} 0.66 & R_{\lambda DL} < 0.45 \\ 0.20R_{\lambda DL} + 0.57 & 0.45 \leq R_{\lambda DL} \leq 1.65 \\ 0.90 & R_{\lambda DL} > 1.65 \end{cases} \tag{5.d}$$

$$D = \begin{cases} 2.00 & R_{\lambda DL} < 0.45 \\ 0.20R_{\lambda DL} + 1.91 & 0.45 \leq R_{\lambda DL} \leq 1.65 \\ 2.24 & R_{\lambda DL} > 1.65 \end{cases} \tag{5.e}$$

$$E = \begin{cases} 0.88 & R_{\lambda DL} < 0.45 \\ 0.35R_{\lambda DL} + 0.72 & 0.45 \leq R_{\lambda DL} \leq 1.65 \\ 1.30 & R_{\lambda DL} > 1.65 \end{cases} \tag{5.f}$$

$$F = \begin{cases} 2.00 & R_{\lambda DL} < 0.55 \\ -0.59R_{\lambda DL} + 2.32 & 0.45 \leq R_{\lambda DL} \leq 1.65 \\ 1.35 & R_{\lambda DL} > 1.65 \end{cases} \tag{5.g}$$

The consideration of the LDG buckling interaction in Equation 5 generates the strength surface solution shown in Figure 4. It can be observed that the resulting surface is a combination of the global strength solution, Equation 1, and the solution presented for LDG, P_{nLDG}, Equation 5.

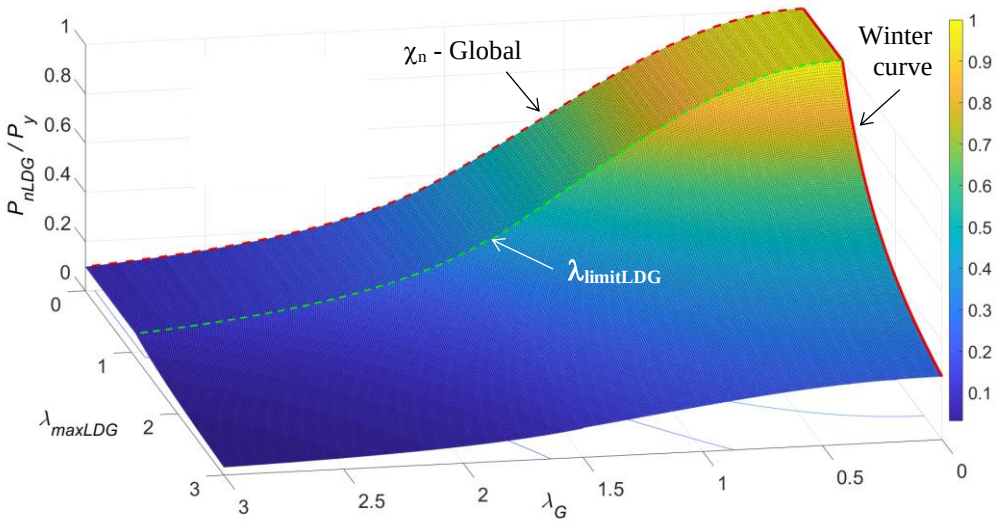

Figure 4: CFS column strength surface described by Equation 5.

Figure 5 shows the comparison between experimental results and the proposed solution for lipped channel columns, including L, D, LD, LG and LDG [24-31,33,34] buckling behavior. These results indicate that the safety criteria proposed by AISI [4] is accomplished, with the LRFD resistance factor $\phi \geq 0.85$. The results were classified according to the reported collapse mode: Local (L), Distortional (D), Local-Distortional interaction (L+D), Local-

Distortional-Flexural Torsional interaction (L+D+FT), Distortional-Flexural Torsional interaction (D+FT), and Global Flexural-Flexural Torsional interaction (F+FT).

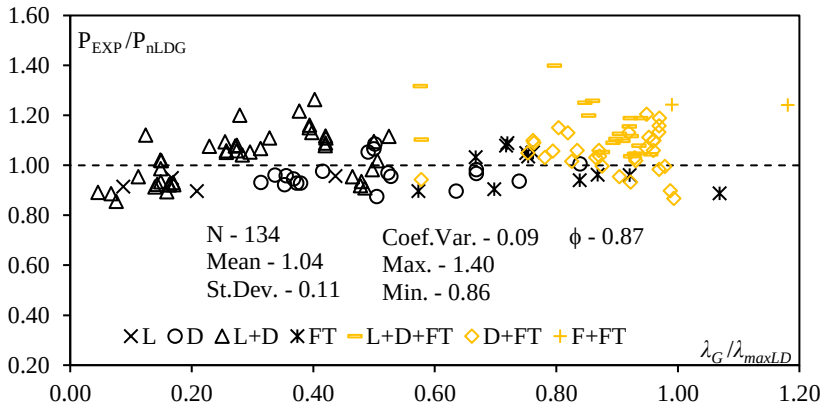

Figure 5 – Comparison between experimental results of lipped channel columns P_{EXP} [24-31,33,34] and the strength surface from Equation 5, P_{nLDG}.

5 Final remarks

The present study demonstrates that LD buckling interaction must be considered for $0.45 \leq R_{\lambda DL} \leq 1.05$, for columns not affected by the global buckling, therefore respecting the slenderness factor ratio $\lambda_G / \lambda_{maxLD} \leq 0.40$. CFS columns out of the range $0.45 \leq R_{\lambda DL} \leq 1.05$ can be designed with the DSM equations related to L or D buckling, Equations 2.a and 2.b, respectively.

The proposed Equation 4 for LD buckling interaction incorporated the slenderness factor ratio, $R_{\lambda DL} = \lambda_D / \lambda_L$, into the calibrated Winter-type solution P_{nLD}. The $R_{\lambda DL}$ parameter estimates the actual possibility of LD interaction, and the strength surface presented in Figure 3 incorporates the columns strength developing L, D and LD buckling. The influence of the global mode was considered with the parameter χ_m in Equation 5, which was derived through a parametric FEM study involving CFS lipped channel columns with significant global mode participation, which means $\lambda_G / \lambda_{maxLD} > 0.40$. The resulting Equation 5 is the DSM-based general procedure which provides accurate estimates of CFS column strength for lipped channel columns, as demonstrated in Figure 5.

Acknowledgements. The first author acknowledges the financial support of CNPq , National Council for Scientific and Technological Research, Brazil, through Doctorate degree scholarship 141287/2019-5.

Authorship statement. The authors hereby confirm that they are the sole liable persons responsible for the authorship of this work, and that all material that has been herein included as part of the present paper is either the property (and authorship) of the authors, or has the permission of the owners to be included here.

References

[1] J.A. Lazzari, E.M. Batista, Finite strip method computer application for buckling analysis of thin-walled structures with arbitrary cross-sections, REM - International Engineering Journal. 74 (2021). https://doi.org/10.1590/0370-44672020740065.
[2] B.W. Schafer, T. Pekoz, Computational modeling of cold-formed steel : characterizing geometric imperfections and residual stresses, 47 (1998) 193–210.
[3] G.J. Hancock, Y.B. Kwon, E. Stefan Bernard, Strength design curves for thin-walled sections undergoing distortional buckling, J Constr Steel Res. 31 (1994) 169–186. https://doi.org/10.1016/0143-974X(94)90009-4.
[4] A.I.A.S. Institute, AISI S100: North American Specification for the Design of Cold-Formed Steel Structural Members, (2016) 505.
[5] AS/NZS (Australian/New Zealand Standard) Cold-Formed Steel Structures – AS/NZS 4600:2018 (3rd ed.), Sydney/Wellington, Australia, 2018.
[6] ABNT, NBR 14762 - Design of cold-formed steel structures (in Portuguese), Rio de Janeiro, Brazil, 2010.
[7] B.W. Schafer, CUFSM 5.04 - Cross-Section Elastic Buckling Analysis: Constrained and Unconstrained Finite Strip Method, Baltimore, USA, 2020.

[8] R. Bebiano, D. Camotim, R. Gonçalves, GBTul 2.0 – a second-generation code for the GBT-based buckling and vibration analysis of thin-walled members, in: Thin-Walled Structures, Lisbon, Portugal, 2018: pp. 235–257.
[9] R.D. Ziemian, Guide to Stability Design Criteria for Metal Structures, 6th Ed., John Wiley & Sons, INC., New York, N. Y., 2010.
[10] American Iron and Steel Institute (AISI) North American Specification (NAS) for the Design of Cold-Formed Steel Structural Members (AISI-S100-16), Washington DC, USA, 2016.
[11] SAS, Theory Reference for the Mechanical APDL and Mechanical Applications, (2009) 1–1226.
[12] G. Matsubara, E. M. Batista, CFS COLUMNS UNDER BUCKLING INTERACTION: DIRECT STRENGTH METHOD GENERALISED APPROACH, in: SDSS 2022, Ernst & sohn, Aveiro, 2022: pp. 1–10.
[13] N. Silvestre, D. Camotim, P.B. Dinis, Post-buckling behaviour and direct strength design of lipped channel columns experiencing local/distortional interaction, J Constr Steel Res. 73 (2012) 12–30. https://doi.org/10.1016/j.jcsr.2012.01.005.
[14] P.B. Dinis, D. Camotim, Cold-formed steel columns undergoing local-distortional coupling: Behaviour and direct strength prediction against interactive failure, Comput Struct. 147 (2015) 181–208. https://doi.org/10.1016/j.compstruc.2014.09.012.
[15] A.D. Martins, D. Camotim, P.B. Dinis, Behaviour and DSM design of stiffened lipped channel columns undergoing local-distortional interaction, J Constr Steel Res. 128 (2017) 99–118. https://doi.org/10.1016/j.jcsr.2016.07.030.
[16] S. Narayanan, M. Mahendran, Ultimate capacity of innovative cold-formed steel columns, J Constr Steel Res. 59 (2003) 489–508. https://doi.org/10.1016/S0143-974X(02)00039-1.
[17] E. Ellobody, B. Young, Behavior of Cold-Formed Steel Plain Angle Columns, Journal of Structural Engineering. 131 (2005) 457–466. https://doi.org/10.1061/(asce)0733-9445(2005)131:3(457).
[18] G.Y. Matsubara, E. M. Batista, G.C. Salles, Lipped channel cold-formed steel columns under local-distortional buckling mode interaction, Thin-Walled Structures. 137 (2019) 251–270. https://doi.org/10.1016/j.tws.2018.12.041.
[19] G.Y. Matsubara, E. M. Batista, Local–distortional buckling mode of steel cold-formed columns: Generalized direct strength design approac, Thin-Walled Structures. 183 (2023), 110356. https://doi.org/10.1016/j.tws.2022.110356.
[20] N. Silvestre, D. Camotim, P.B. Dinis, Post-buckling behaviour and direct strength design of lipped channel columns experiencing local/distortional interaction, J Constr Steel Res. 73 (2012) 12–30. https://doi.org/10.1016/j.jcsr.2012.01.005.
[21] P.B. Dinis, D. Camotim, Cold-formed steel columns undergoing local-distortional coupling: Behaviour and direct strength prediction against interactive failure, Comput Struct. 147 (2015) 181–208. https://doi.org/10.1016/j.compstruc.2014.09.012.
[22] Landesmann, D. Camotim, On the Direct Strength Method (DSM) design of cold-formed steel columns against distortional failure, Thin-Walled Structures. 67 (2013) 168–187. https://doi.org/10.1016/j.tws.2013.01.016.
[23] A.D. Martins, P.B. Dinis, D. Camotim, P. Providência, On the relevance of local-distortional interaction effects in the behaviour and design of cold-formed steel columns, Comput Struct. 160 (2015) 57–89. https://doi.org/10.1016/j.compstruc.2015.08.003.
[24] B. Young, N. Silvestre, D. Camotim, Cold-Formed Steel Lipped Channel Columns Influenced by Local-Distortional Interaction: Strength and DSM Design, Journal of Structural Engineering. 139 (2013) 1059–1074. https://doi.org/10.1061/(asce)st.1943-541x.0000694.
[25] B. Young, K.J.R. Rasmussen, Design of lipped channel columns, Journal of Structural Engineering. 124 (1998) 140–148. https://doi.org/10.1061/(ASCE)0733-9445(1998)124:2(140).
[26] Y.B. Kwon, G.J. Hancock, Tests of cold-formed channels with local and distortional buckling, Journal of Structural Engineering. 118 (1992) 1786–1803.
[27] J. Loughlan, N. Yidris, K. Jones, The failure of thin-walled lipped channel compression members due to coupled local-distortional interactions and material yielding, Thin-Walled Structures. 61 (2012) 14–21. https://doi.org/10.1016/j.tws.2012.03.025.
[28] S.C.W. Lau, G.J. Hancock, Distortional buckling tests of cold-formed channel sections., in: Ninth International Specialty Conference on Cold-Formed Steel Structures, St. Louis, Missouri, USA, 1988: pp. 45–78.
[29] J. Chen, M.-T. Chen, B. Young, Compression Tests of Cold-Formed Steel C- and Z-Sections with Different Stiffeners, Journal of Structural Engineering. 145 (2019) 04019022. https://doi.org/10.1061/(asce)st.1943-541x.0002305.
[30] L. Huang, W. Yang, T. Shi, J. Qu, Local and Distortional Interaction Buckling of Cold-formed Thin-Walled High Strength Lipped Channel Columns, International Journal of Steel Structures. 21 (2021) 244–259. https://doi.org/10.1007/s13296-020-00436-z.
[31] J. Chen, M.-T. Chen, B. Young, Compression Tests of Cold-Formed Steel C- and Z-Sections with Different Stiffeners, Journal of Structural Engineering. 145 (2019) 04019022. https://doi.org/10.1061/(asce)st.1943-541x.0002305.
[32] R.G.A. Campos, Análise da interação entre os modos de flambagem local e distorcional em perfis de aço formados a frio com seção rack sob compressão axial, Master Thesis (in Portuguese). Federal University of Rio de Janeiro, Rio de Janeiro, Brazil, 2020.
[33] E. Souza dos Santos, E. M. Batista, D. Camotim, Cold-formed steel columns under L-D-G interaction, Steel Construction. 7 (2014) 193–198. https://doi.org/10.1002/stco.201410034.
[34] B. Young, P.B. Dinis, D. Camotim, CFS lipped channel columns affected by L-D-G interaction. Part I: Experimental investigation, Comput Struct. 207 (2018) 219–232. https://doi.org/10.1016/j.compstruc.2017.03.016.